Shock Boundary Interactions Generated By The Fin On A Semi-cylindrical Body

Jiawei Sun[1]

[1]Department of Mechanical and Aerospace Engineering, Tandon School of Engineering, New York University, Brookly, NY, USA.

Abstract

This study investigates the shock boundary layer interaction occurring at the base of a double sharp fin. The base geometry is of particular interest, with comparisons made between flat and semi-cylindrical bases. The flow field is characterized via numerical simulations and identifications of vortices in the flow field are made. There have been many studies on the shock boundary layer interaction generated by fins located on flat surfaces, but relatively few on fins located on semi-cylindrical surfaces.
It is observed in supersonic flow past a fin that the fluid in the contact region between the fin's root and the semi-cylinder exhibits turbulent phenomena, and the angle between the shock wave and the fin will decrease continuously as the Mach number increases. The separation shock will continuously move towards the fin root, and the vortex generated by the fin will reduce the speed of the fluid passing over the surface of the fin. After comparing separation vortices generated by plate-based fins and semi-cylinder fins, vortices generated by both the downwind fin and upwind fin rotate in the same direction in the semi-cylinder fin model, but separation vortices will change direction in downwind plate-based fin model. For the downwind plate-based fin, separation vortices will rise near the fin and descend far from the fin.
Further examination of the relationship between the Strouhal number and the Reynolds number will assist designers in predicting the behavior of aircraft under different speed conditions.

Reference

[1] Fage, A., & Sargent, R. F. (1947). Shock-wave and boundary-layer phenomena near a flat surface. Proceedings of the Royal Society of London. Series A, Mathematical and Physical Sciences, 190(1020), 1–20. https://doi.org/10.1098/rspa.1947.0058.
[2] Barry, F. W., Shapiro, A. H., & Neumann, E. P. (1950). Some Experiments on the Interaction of Shock Waves With Boundary Layers on a Flat Plate. Journal of Applied Mechanics, 17(2), 126–131. https://doi.org/10.1115/1.4010089.
[3] Yasuhara Michiru. (1957). On the Hypersonic Viscous Flow past a Flat Plate with Suction or Injection. Journal of the Physical Society of Japan, 12(2), 177–182.
[4] Keenan, J. H., & Neumann, E. P. (1946). Measurements of Friction in a Pipe for Subsonic and Supersonic Flow of Air. Journal of Applied Mechanics, 13(2), A91–A100. https://doi.org/10.1115/1.4009532.
[5] Bershader, D. (1949). An Interferometric Study of Supersonic Channel Flow. Review of Scientific Instruments, 20(4), 260–275. https://doi.org/10.1063/1.1741506.
[6] Kaye, J., Keenan, J. H., Klingensmith, K. K., Ketchum, G. M., & Toong, T. Y. (1952). Measurement of Recovery Factors and Friction Coefficients for Supersonic Flow of Air in a Tube: 1—Apparatus, Data, and Results Based on a Simple One-Dimensional Flow Model. Journal of Applied Mechanics, 19(1), 77–96. https://doi.org/10.1115/1.4010410.

[7] Wachtell, G. P., & Carfagno, S. P. (1959). Supersonic Flow in a Tube with Longitudinal Slots. The Physics of Fluids (1958), 2(5), 521–526. https://doi.org/10.1063/1.1705943.
[8] Kuethe, A. M., Ishii, T., & Amick, J. L. (1964). Boundary-Layer Transition on a Cooled Rough Sphere in Hypersonic Flow. The Physics of Fluids (1958), 7(8), 1198–1200. https://doi.org/10.1063/1.1711361.
[9] Kim, C.-S. (1959). Experimental Studies on the Hypersonic Flow past Plate, Convex and Concave Wedges. Journal of the Physical Society of Japan, 14(6), 827–837. https://doi.org/10.1143/JPSJ.14.727.
[10] Fang, J., Yao, Y., Zheltovodov, A. A., & Lu, L. (2017). Investigation of Three-Dimensional Shock Wave/Turbulent-Boundary-Layer Interaction Initiated by a Single Fin. AIAA Journal, 55(2), 509–523. https://doi.org/10.2514/1.J055283.
[11] Wang, L., Zhao, Y., Wang, Q., Zhao, Y., Zhang, R., & Ma, L. (2022). Three-dimensional characteristics of crossing shock wave/turbulent boundary layer interaction in a double fin with and without micro-ramp control. AIP Advances, 12(9), 095309-095309–095314. https://doi.org/10.1063/5.0102986.
[12] Otten, D. L., & Lu, F. K. (2022). Flow features of swept shock/turbulent boundary-layer interaction due to a gap beneath a sharp fin. Aerospace Science and Technology, 130, 107934-. https://doi.org/10.1016/j.ast.2022.107934.
[13] Eitner, M. A., Ahn, Y.-J., Musta, M. N., Clemens, N. T., & Sirohi, J. (2023). Vibration of a thin panel exposed to ramp-induced shock-boundary layer interaction at Mach 2. Journal of Fluids and Structures, 119, 103894-. https://doi.org/10.1016/j.jfluidstructs.2023.103894.
[14] Zhou, Y. Y., Zhao, Y. L., He, G., Zhao, Y. X., & Gao, P. Y. (2023). Study on the separation in the shock wave/boundary layer interaction induced by a curved fin. Physics of Fluids (1994), 35(7). https://doi.org/10.1063/5.0155076.
[15] Y. Zhao, Y. Zhou, G. He and Y. Zhao. (2023). Visualization of shock-free compression/laminar boundary layer interaction caused by a curved fin in supersonic flow, 17th Asian Congress of Fluid Mechanics (ACFM 2023), 24-29, doi: 10.1049/icp.2023.1924.
[16] GANG, D., YI, S., ZHANG, F., & NIU, H. (2022). Effects of sweep angles on turbulent separation behaviors induced by blunt fin. Chinese Journal of Aeronautics, 35(3), 90–97. https://doi.org/10.1016/j.cja.2021.03.032.
[17] Baldwin, A., Mears, L. J., Kumar, R., & Alvi, F. S. (2021). Effects of Reynolds Number on Swept Shock-Wave/Boundary-Layer Interactions. AIAA Journal, 59(10), 3883–3899. https://doi.org/10.2514/1.J060293.
[18] Pickles, J. D., & Narayanaswamy, V. (2020). Control of Fin Shock Induced Flow Separation Using Vortex Generators. AIAA Journal, 58(11), 4794–4806. https://doi.org/10.2514/1.J059624.
[19] McCormick, D. C. (1993). Shock/boundary-layer interaction control with vortex generators and passive cavity. AIAA Journal, 31(1), 91–96. https://doi.org/10.2514/3.11323.
[20] Gaitonde, D. V., & Adler, M. C. (2023). Dynamics of Three-Dimensional Shock-Wave/Boundary-Layer Interactions. Annual Review of Fluid Mechanics, 55(1), 291–321. https://doi.org/10.1146/annurev-fluid-120720-022542.
[21] Bruno, O. P., Cubillos, M., & Jimenez, E. (2019). Higher-order implicit-explicit multi-domain compressible Navier-Stokes solvers. Journal of Computational Physics, 391, 322–346. https://doi.org/10.1016/j.jcp.2019.02.033.
[22] Nived, M. R., Athkuri, S. S. C., & Eswaran, V. (2022). On the application of higher-order Backward Difference (BDF) methods for computing turbulent flows. Computers & Mathematics with Applications (1987), 117, 299–311. https://doi.org/10.1016/j.camwa.2022.05.007.
[23] Schenk, O., Gärtner, K., Fichtner, W., & Stricker, A. (2001). PARDISO: a high-performance serial and parallel sparse linear solver in semiconductor device simulation. Future Generation Computer Systems, 18(1), 69–78. https://doi.org/10.1016/S0167-739X(00)00076-5.
[24] NASA Langley Research Center Turbulence Modeling Resource, 3D ONERA M6 Wing Validation Case, https://turbmodels.larc.nasa.gov/onerawingnumerics_val.html
[25] Yu, N. J. (1980). Efficient Transonic Shock-Free Wing Redesign Procedure Using a

Fictitious Gas Method. AIAA Journal, 18(2), 143–148. https://doi.org/10.2514/3.50744.
[26] Zhang, Y., Han, Z., & Song, W. (2024). Multi-fidelity expected improvement based on multi-level hierarchical kriging model for efficient aerodynamic design optimization. Engineering Optimization. https://doi.org/10.1080/0305215X.2024.2310182.

Figures used in the abstract

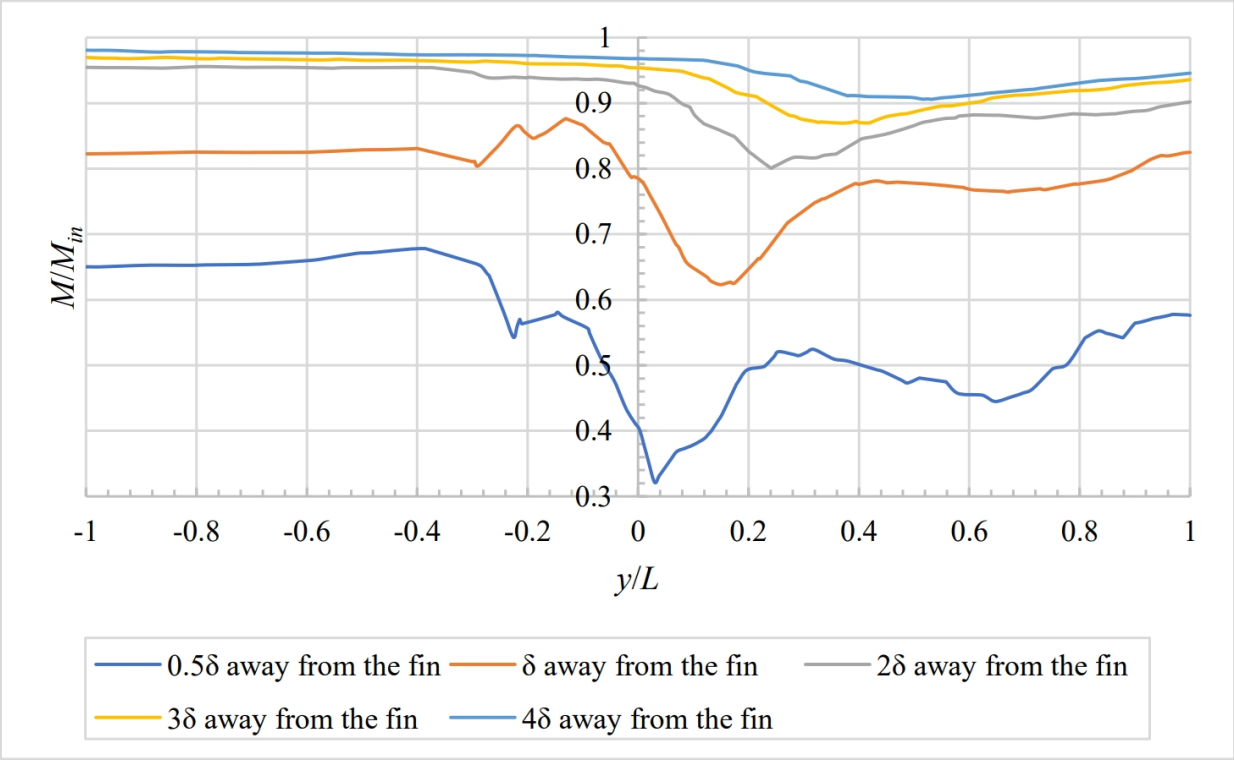

Figure 4.12c: Change in Mach number along the parallel line with the fin ($M_{in} = 2.7$).

Figure 1

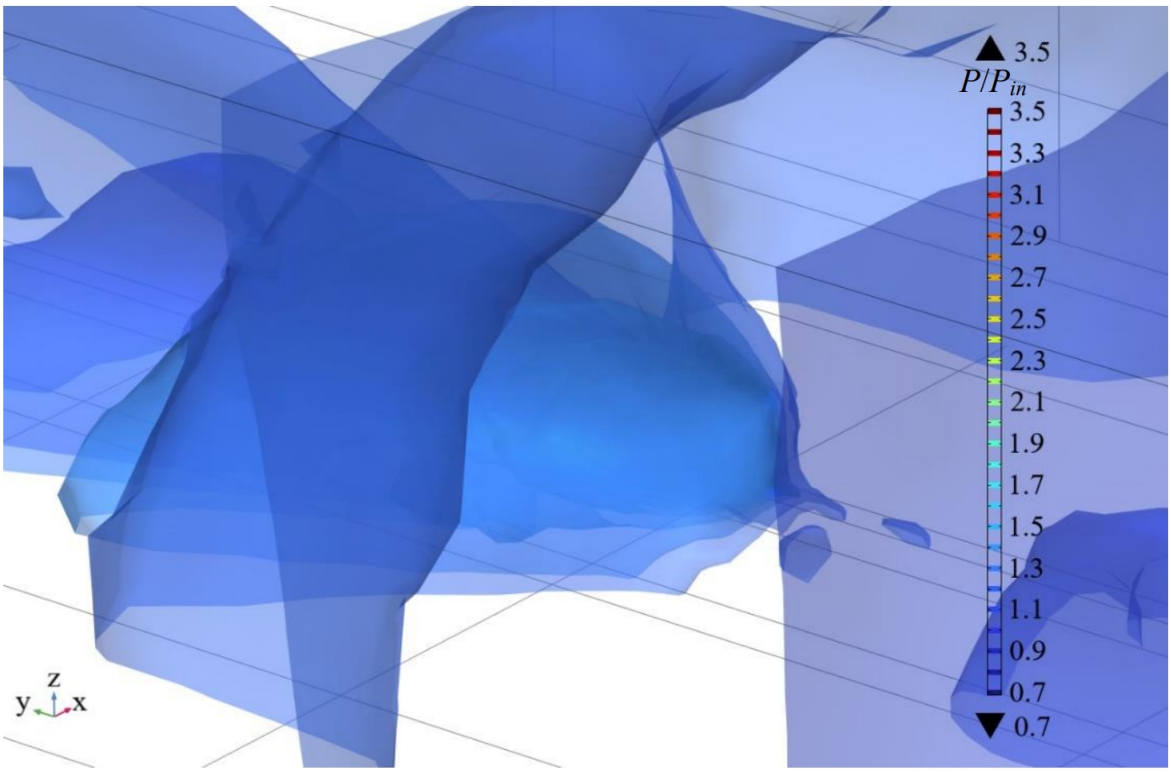

Figure 4.9b: Pressure contours, orientation in Figure 2.1b (fin on cylinder) (M_{in} = 3.0).

Figure 2

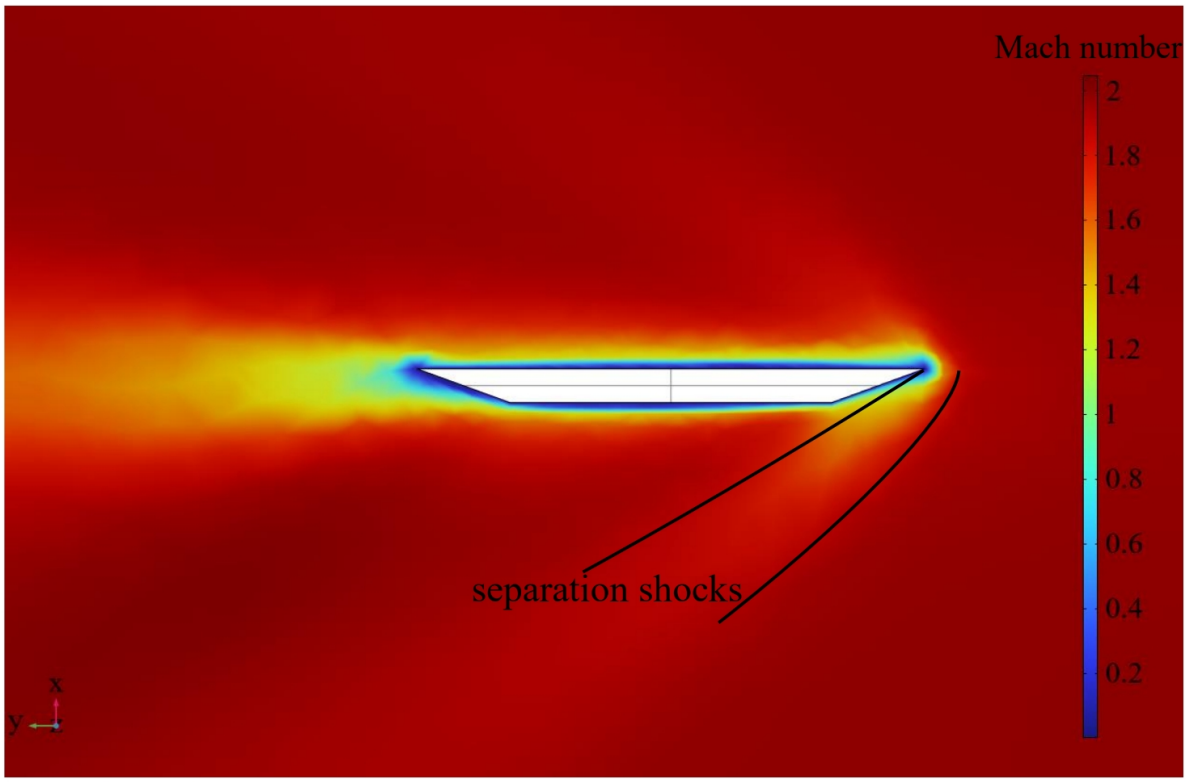

Figure 4.11a: Separation shocks and Mach number contour surface on the horizontal slice at the root of the fin (fin on cylinder) (M_{in} = 2.0).

Figure 3

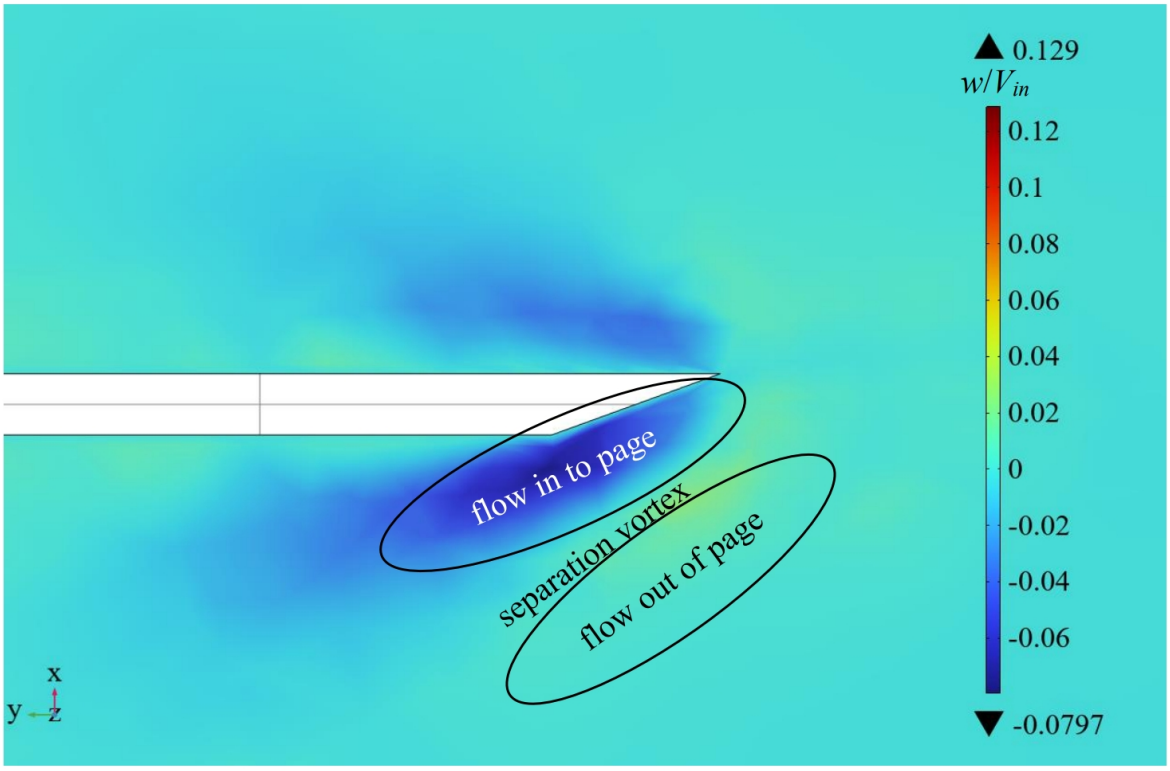

Figure 4.6: Spanwise velocity distribution generated by the fin on cylinder, upwind fin (M_{in} = 2.7).

Figure 4